Chin. J. Mech. Eng. (2017) 30:1325–1337
https://doi.org/10.1007/s10033-017-0187-0

ORIGINAL ARTICLE

Online Condition Monitoring of Gripper Cylinder in TBM Based on EMD Method

Lin Li[1] · Jian-Feng Tao[1] · Hai-Dong Yu[2] · Yi-Xiang Huang[1] · Cheng-Liang Liu[1]

Received: 29 November 2016 / Revised: 2 August 2017 / Accepted: 29 September 2017 / Published online: 31 October 2017

Abstract The gripper cylinder that provides braced force for Tunnel Boring Machine (TBM) might fail due to severe vibration when the TBM excavates in the tunnel. Early fault diagnosis of the gripper cylinder is important for the safety and efficiency of the whole tunneling project. In this paper, an online condition monitoring system based on the Empirical Mode Decomposition (EMD) method is established for fault diagnosis of the gripper cylinder while TBM is working. Firstly, the lumped mass parameter model of the gripper cylinder is established considering the influence of the variable stiffness at the rock interface, the equivalent stiffness of the oil, the seals, and the copper guide sleeve. The dynamic performance of the gripper cylinder is investigated to provide basis for its health condition evaluation. Then, the EMD method is applied to identify the characteristic frequencies of the gripper cylinder for fault diagnosis and a field test is used to verify the accuracy of the EMD method for detection of the characteristic frequencies. Furthermore, the contact stiffness at the interface between the barrel and the rod is calculated with Hertz theory and the relationship between the natural frequency and the stiffness varying with the health condition of the cylinder is simulated based on the dynamic model. The simulation shows that the characteristic frequencies decrease with the increasing clearance between the barrel and the rod, thus the defects could be indicated by monitoring the natural frequency. Finally, a health condition management system of the gripper cylinder based on the vibration signal and the EMD method is established, which could ensure the safety of TBM.

Keywords Fault diagnosis · Empirical mode decomposition (EMD) · Condition Monitoring · Gripper cylinder · TBM

1 Introduction

Tunnel boring machine (TBM) is widely used for underground construction due to the higher efficiency and better quality of the tunnel in recent decades. However, the TBM suffers strong vibration that could cause failure of its main components, such as fracture of the cutters, leakage of the cylinders, and initiation of cracks on the main bearing. The gripper cylinder providing braced force is used for keeping the TBM stable and direction adjustment. The wear and fracture of the seals or Copper Guide Sleeve (CGS) would cause failure of the gripper cylinder, which result in shutdown of the TBM for lacking sufficient braced force. It takes long time to prepare and change the gripper cylinder, thus early fault diagnosis of the gripper cylinder is important for the safety and efficiency of the tunnel construction.

The dynamic characteristics are the basement for fault diagnosis of different mechanical systems by means of vibration signals. The vibration performance has been analysed for the strength estimation or life prediction of TBM [1–3]. A multi-directional coupling dynamic model

Supported by National Basic Research Program of China (Grant No. 2013CB035403), National Natural Science Foundation of China (Grant No. 51375297) and Program of Shanghai Subject Chief Scientist of China (Grant No. 14XD1402000).

✉ Jian-Feng Tao
jftao@sjtu.edu.cn

[1] State Key Laboratory of Mechanical System and Vibration, Shanghai Jiao Tong University, Shanghai 200240, China

[2] Shanghai Key Laboratory of Digital Manufacture for Thin-walled Structures, Shanghai 200240, China

was established to analyse the dynamic characteristics of the cutterhead system in TBM. Different working parameters were studied to find out the optimization scheme for the cutterhead structure [1]. Zhang et al. [4] presented a dynamic model for the TBM revolving system considering the periodically varying mesh stiffness of the multiple pinions and the speed-torque characteristics of the variable frequency motor. The result showed the excavation torque could run up to a critical value in the extremely adverse excavation environments, which might result in an unexpected breakdown of TBM and even a failure of the drive motor. A multi-freedom coupling dynamic model for the cutterhead system was established to investigate its natural frequencies and vibration modes [5]. The model laid the foundation for the dynamic performance optimization and fatigue life prediction for the cutterhead system. Zou et al. [6] proposed a dynamic model for the main machine of TBM that included the cutterhead, the driving system, the thrust system, and the interaction between the TBM and the surrounding rocks in terms of the lump parameter method. Different researches show that vibration of TBM could influence the efficiency and the fatigue life of different components, especially the cutterhead and the main drive motor. However, the gripper cylinder is also vulnerable to the vibration which might be neglected. In this paper, the dynamic model of the gripper cylinder is established to analyse its vibration performance with degeneration of health condition.

Vibration signals are the most common monitoring parameters for health management of mechanical system. The traditional signal processing methods, such as Fast Fourier Transformation (FFT) and spectrum analysis, are merely able to obtain the basic frequency of the stationary signal. However, the vibration signals acquired from the working machines that contain complex noises are usually non-stationary and nonlinear. Hence, the frequencies are commonly mixed and the fault features are difficult to be identified from the raw signals. The time–frequency domain analysis methods, such as Short Time Fourier Transform (STFT), Wigner–Ville Distribution (WVD) and Wavelet Transform Analysis (WTA), are proposed to deal with the non-stationary signals [7–9]. In recent years, the Empirical Mode Decomposition (EMD) [10] method has been widely used for fault diagnosis of mechanical systems because it is self-adaptive and no basis is required in advance. Lei et al. [11] concluded that the EMD method was applicable for condition monitoring of numerous rotational components, such as gears, bearings,and motors. The instantaneous frequency could be calculated for fault characteristic frequency detection when the vibration signals are decomposed into a series of Intrinsic Mode Functions (IMFs). The traditional EMD algorithm has several disadvantages, such as the mixing mode, the end effect, and the physical meanings of IMFs are not clear. Thus, researchers proposed several new algorithms to overcome these feedbacks [12–15]. Yan et al. [16] presented a weak signal detection method based on the improved Hilbert-Huang Transform (HHT) by restraining the end effect of the traditional EMD method. The improved HHT method combined with the wavelet analysis had a satisfactory performance for weak signal analysis and it could diagnose the incipient rotor imbalance of the Bently test-rig. An improved Extended EMD (EEMD) method was used for analysing the short hydraulic impact signals besides the application of EMD method in vibration signals. The fault diagnosis approach combining with the improved EEMD method and the Support Vector Machine (SVM) classification algorithm was proved to be propitious for fault diagnosis in hydraulic system [17]. Saidi et al. [18] proposed a Bi-Spectrum based EMD (BSEMD) method to improve the fault diagnosis performance of the traditional EMD method. The outer race bearing defects could be detected with the bi-spectrum analysis of the decomposed IMFs and the health condition of the bearing could be assessed. The studies show that the EMD method is powerful for fault diagnosis in the mechanical system, thus it is chosen to indicate the failure of the gripper cylinder in TBM.

The gripper cylinder is important for balancing the external loads from the cutterhead and keeping the main machine stable. Thus, early fault diagnosis for the gripper cylinder is significant. In this paper, an online condition monitoring system for the gripper cylinder is proposed with the application of the EMD method, which is based on the dynamic model. The remainder of this paper is shown as follows. A lumped mass parameter model of the gripper cylinder is established and the characteristic frequencies are calculated in Section 2. Section 3 illustrates the principle of the EMD method and verifies the accuracy of the algorithm. In Section 4, the EMD method is applied for analysing the nonlinear and non-stationary signal acquired from one type of TBM to indicate the characteristic frequencies. Moreover, the relationship between the equivalent stiffness and the characteristic frequency is simulated. Finally, an online condition monitoring system is established for health condition evaluation of gripper cylinder. The conclusions are drawn in Section 5.

2 Dynamic Analysis of the Gripper Cylinder in TBM

2.1 Dynamic Model of the Gripper Cylinder in TBM

Figure 1 shows that the main machine of TBM is consisted of the cutterhead system, the main drive containing the bearings and the motors, the thrust cylinders, the

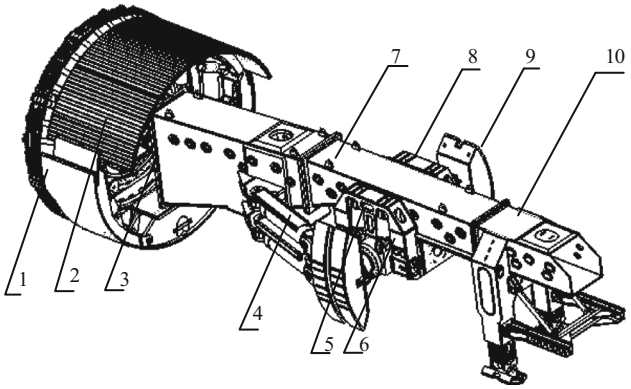

1.Cutterhead System; 2. Forward Shield; 3. Main drive; 4. Thrust cylinder; 5.Torque Cylinder ; 6. Gripper Cylinder; 7. Main Girder; 8.Saddle; 9. Gripper Shoes; 10.Back Side Support

Figure 1 Structure of the main machine for TBM

gripper cylinder and the other auxiliary components. The working flow illustrating the boring loops of TBM is shown in Figure 2. Firstly, the gripper cylinder (6) extends to support the gripper shoes (8) onto the rock for providing braced force and keeping the main machine stable. The gripper cylinder is connected with the main girder (7) with four torque cylinders (5). The gripper cylinder and the torque cylinder are used for balancing the tunneling loads. Then, the thrust cylinder would propel the cutterhead system to cut and crush the rocks.

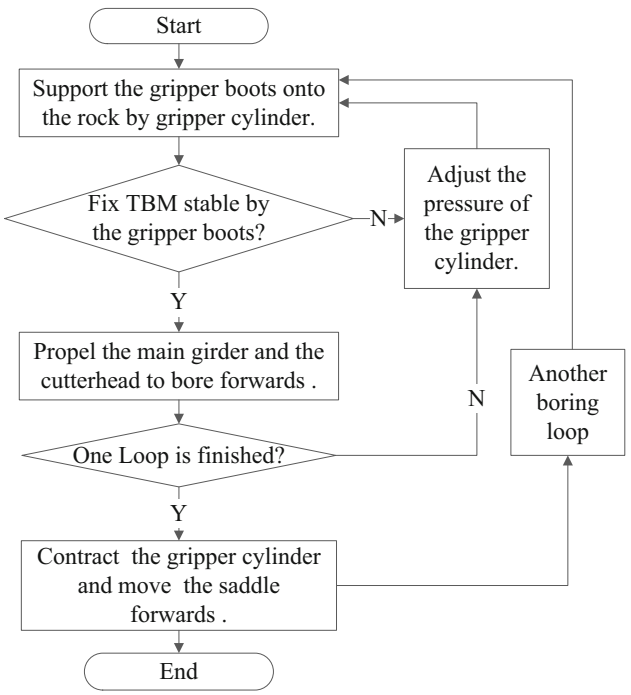

Figure 2 Workflow for tunneling

In addition, the boring direction can be adjusted by changing the inlet pressures of different chambers in the gripper cylinder. Hence, the TBM cannot work if the gripper cylinder has defects because it fails to obtain enough braced force and change boring direction.

The gripper cylinder contains two asymmetrical single rod cylinders and the chambers without piston rods are connected with each other by pipelines. The structure of the asymmetrical single rod cylinder is shown in Figure 3 and it is consisted of the barrel, the piston rod, the CGS, the seals, the gland and the other accessories.

A six-degree lumped mass parameter model of gripper cylinder can be obtained as illustrated in Fig. 4 because the CGS and the seals have the same velocity with the piston rod. Set the origin of the coordinate system at the centre of the rod. The axial displacements of the barrel and the rod are represented by x_1 and x_2, the radial displacements of the barrel and rod are denoted as y_1 and y_2, meanwhile the bending angles are θ_1 and θ_2, respectively. The cylinder barrel and the rod are equivalent as rigid beams with the barycenter in their middle and they are represented with m_b and m_r. The lengths of the barrel and the rod are L_b and L_r. Their bending moments are $I_b = 1/2m_bL_b^2$ and $I_r = 1/2m_rL_r^2$, respectively. The seals and the CGS are regarded as point masses at the end of the piston rod that are denoted as m_s and m_c. Moreover, a_1 represents the distance between the centre of the barrel and the seals, and a_2 is the distance between the centre of the rod and the CGS. The interaction between the gripper boots and the rocks is considered as the equivalent stiffness of the rock represented by k_r that is combined with the normal contact stiffness and the tangential contact stiffness. In addition, the equivalent stiffness of the seals, the CGS, the oil, and

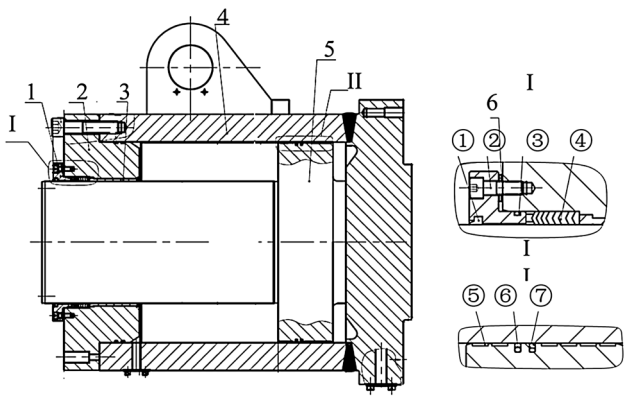

1.Gland; 2.Guide sleeve; 3. Copper guide sleeve;4. Barrel; 5.Piston rod;10.Seals at rod end; 6.Adjusting shim; ①Scraper seal; ②Inner hexagon screw; ③O ring; ④ Seals at rod end; ⑤ Guide sleeve; ⑥,⑦ Seals for hole;

Figure 3 Structure of the gripper cylinder

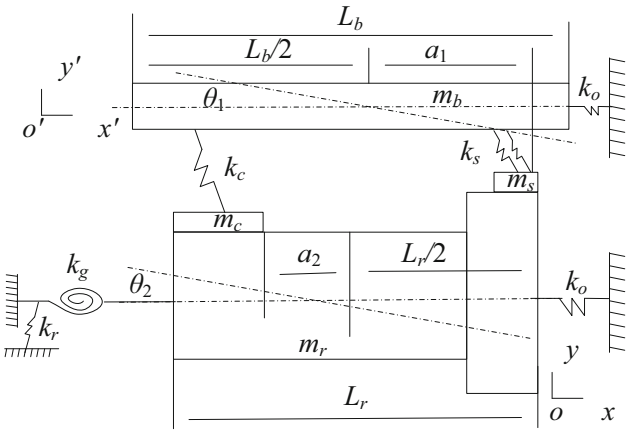

Figure 4 The lumped parameter model of gripper cylinder

the bending stiffness of gripper are regarded as k_s, k_c, k_o and k_g, respectively. The external axial forces are represented by F_1, F_2, the radial forces are denoted as F_3, F_4 and the torque of the barrel and the rod are M_1, M_2, respectively.

Based on the lumped mass parameter model of the gripper cylinder, the kinetic energy T of the system is

$$\begin{aligned} T = {} & \frac{1}{2}m_b\dot{y}_1^2+\frac{1}{2}m_b\dot{x}_1^2+\frac{1}{2}I_b\dot{\theta}_1^2 \\ & +\frac{1}{2}m_c\left[\left(\dot{y}_2+\frac{L_r}{2}\dot{\theta}_2\right)^2+\dot{x}_2^2\right]+\frac{1}{2}m_r\dot{y}_2^2 \\ & +\frac{1}{2}m_r\dot{x}_2^2+\frac{1}{2}I_r\dot{\theta}_2^2+\frac{1}{2}m_s\left[\left(\dot{y}_2-\frac{L_r}{2}\dot{\theta}_2\right)^2+\dot{x}_2^2\right], \end{aligned} \tag{1}$$

and the potential energy V of the system is

$$\begin{aligned} V = {} & \frac{1}{2}k_s\left\{\left[(y_1-a_1\theta_1)-\left(y_2-\frac{L_r}{2}\theta_2\right)\right]^2+(x_1-x_2)^2\right\} \\ & +\frac{1}{2}k_c\left\{\left[\left(y_1+\frac{L_b}{2}\theta_1\right)-(y_2+a_2\theta_2)\right]^2+(x_1-x_2)^2\right\} \\ & +\frac{1}{2}k_o((x_1-x_2)^2+(y_1-y_2)^2)+\frac{1}{2}k_s(y_2^2+x_2^2)+\frac{1}{2}k_g\theta_2^2. \end{aligned} \tag{2}$$

Suppose $\boldsymbol{q} = [x_1,\ y_1,\ \theta_1,\ x_2,\ y_2,\ \theta_2]^{\mathrm{T}}$ is a vector containing the system coordinates, in which q_i are the generalized coordinates of the systems and $\dot{q}_i$ are the generalized velocities, Q_i is the total generalized forces that are not related to the potential energy of the system.

According to $\mathrm{d}y/\mathrm{d}t(\partial L/\partial\dot{q}_i)-\partial L/\partial q_i = Q_i$, where $L = T - V$, the vibration equations of the gripper cylinder system can be expressed as Eq. (3) under the circumstance that the damping behaviour is neglected.

$$\boldsymbol{M}\ddot{\boldsymbol{q}}+\boldsymbol{K}\boldsymbol{q} = \boldsymbol{0}, \tag{3}$$

where $\boldsymbol{M}$, $\boldsymbol{K}$ and $\boldsymbol{F}$ stand for mass matrix, stiffness matrix and force vector, respectively. The details of the mass matrix, the stiffness matrix and force vector are presented as follows:

$$\boldsymbol{M} = \begin{bmatrix} \boldsymbol{M_{11}} & \boldsymbol{M_{12}} \\ \boldsymbol{M_{21}} & \boldsymbol{M_{22}} \end{bmatrix},\ \boldsymbol{K} = \begin{bmatrix} \boldsymbol{K_{11}} & \boldsymbol{K_{12}} \\ \boldsymbol{K_{21}} & \boldsymbol{K_{22}} \end{bmatrix}, \tag{4}$$

$$\boldsymbol{F} = [F_1, F_2, M_1, F_3, F_4, M_2]^{\mathrm{T}}, \tag{5}$$

$$\boldsymbol{M_{11}} = \begin{bmatrix} m_b & & \\ & m_b & \\ & & I_b \end{bmatrix},\ \boldsymbol{M_{12}} = \boldsymbol{M_{21}} = \boldsymbol{0}, \tag{6}$$

$$\boldsymbol{M_{22}} = \begin{bmatrix} m_r+m_c+m_s & 0 & 0 \\ 0 & m_r+m_c+m_s & \frac{L_rm_c}{2}-\frac{L_rm_s}{2} \\ 0 & \frac{L_rm_c}{2}-\frac{L_rm_s}{2} & I_r+\frac{L_r^2m_c}{4}+\frac{L_r^2m_s}{4} \end{bmatrix}, \tag{7}$$

$$\boldsymbol{K_{11}} = \begin{bmatrix} k_o+k_s+k_c & 0 & 0 \\ 0 & k_o+k_s+k_c & -a_1k_s+\frac{L_bk_c}{2} \\ 0 & -a_1k_s+\frac{L_bk_c}{2} & a_1^2k_s+\frac{L_b^2k_c}{4} \end{bmatrix}, \tag{8}$$

$$\boldsymbol{K_{12}} = \boldsymbol{K_{21}} = \begin{bmatrix} -(k_o+k_c+k_s) & 0 & 0 \\ 0 & -(k_o+k_c+k_s) & a_1k_s-\frac{L_bk_c}{2} \\ 0 & -a_2k_c+\frac{L_rk_s}{2} & -\frac{a_1L_rk_s+a_2L_bk_c}{2} \end{bmatrix}, \tag{9}$$

$$\boldsymbol{K_{22}} = \begin{bmatrix} k_r+k_o+k_c+k_s & 0 & 0 \\ 0 & k_s+k_c-k_o+k_r & -\frac{L_rk_s}{2}+a_2k_c \\ 0 & -\frac{L_rk_s}{2}+a_2k_c & k_g+a_2^2k_c+\frac{L_r^2k_s}{4} \end{bmatrix}. \tag{10}$$

2.2 Simulation of the Dynamic Model

The values of different equivalent stiffness in the dynamic model and the parameters of the gripper cylinder in the TBM used for field test are illustrated in Table 1. The vibration displacements of the gripper cylinder are calculated and they are shown in Figure 5. The radial displacements amplitudes of the barrel and rod are near to 0.04 mm and 0.03 mm, respectively. Moreover, the amplitudes of the axial displacements of the barrel and the rod are 0.08 mm and 0.03 mm, respectively. The bending displacement of the barrel is 0.1 rad and the bending displacement of the rod is almost 0 rad since the gripper is against to the rock and the bending stiffness prevents the rod from bending too much.

Table 1 Parameters of masses and equivalent stiffness

Equivalent stiffness	Value (GN/m)	Mass	Value (kg)
Hydraulic Oil	0.3	Barrel	5374
Contact stiffness of CGS	0.2	Rod	2810
Contact stiffness of seals	0.1	Seals	0.02
Contact stiffness of rock	20	CGS	5.01
Bending stiffness	3/rad		

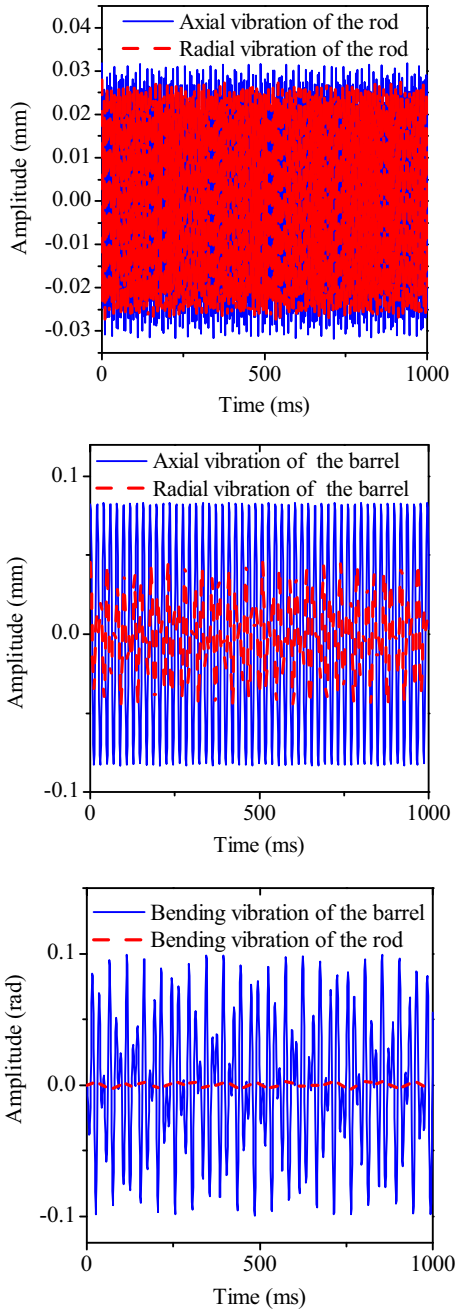

Figure 5 Dynamic performance of gripper cylinder

The characteristic frequencies of the gripper cylinder are calculated and the results are illustrated in Figure 6. The natural frequencies of the barrel the rod are 51.3 Hz and 214.8 Hz for the axial vibration, respectively. The natural frequencies of the barrel the rod are 39.3 Hz and 214.8 Hz for the axial vibration, respectively. The frequencies of the bending vibration of the barrel are 39.3 Hz and 60.9 Hz and the bending vibration of the rod are more complex with the frequencies of 39.3 Hz, 60.9 Hz, 78.3 Hz and 214.8 Hz. The results show that the radial vibration and the bending vibration of the barrel are coupled with each other. In addition, the radial, the axial vibration and the bending vibration of the rod are mixed.

3 Principle of EMD Method

The EMD method is powerful for time–frequency analysis and it is widely used in signal processing [19–21]. A signal can be decomposed into a series of IMFs that represent basic oscillatory modes imbedded in the signal by EMD method [10]. The steps of the original EMD algorithm are illustrated in Figure 7. Firstly, the local maxima and minimum of the signal, $x(t)$, are calculated, then the cubic spline interpolation is used to obtain the maxima and minima envelope. The mean value of the maxima and minima envelope is defined as m_1. Consequently, the first component h_1 could be obtained by subtracting m_1 from $x(t)$ and h_1 could be an IMF in the ideal condition. However, the signal is usually complicated, therefore, a "sieve" is always used to get rid of mixed waves and to make the waves more symmetrical to get the true IMF in the actual practice [22].

Assuming h_1 is the original signal, a temporary IMF represented with h_{11} could be obtained with a cyclic of the mentioned steps,

$$h_1 - m_{11} = h_{11}, \tag{11}$$

then the true intrinsic mode function (IMF) denoted as h_{1k} could be calculated by repeating the steps k times,

$$h_{1(k-1)} - m_{1k} = h_{1k}. \tag{12}$$

The standard deviation (SD) that is in a range of 0.2–0.3 between two "sieves" is calculated to stop the loop and the SD is expressed as

$$SD = \sum_{t=0}^{T} \left[\frac{\left| h_{1(k-1)}(t) - h_{1k}(t) \right|^2}{h_{1(k-1)}^2(t)} \right]. \tag{13}$$

The first IMF h_{1k} that includes the minima scale or the shortest period of the original signal is separated from the signal until SD reaches the set value and it could be expressed as

$$c_1 = h_{1k}. \tag{14}$$

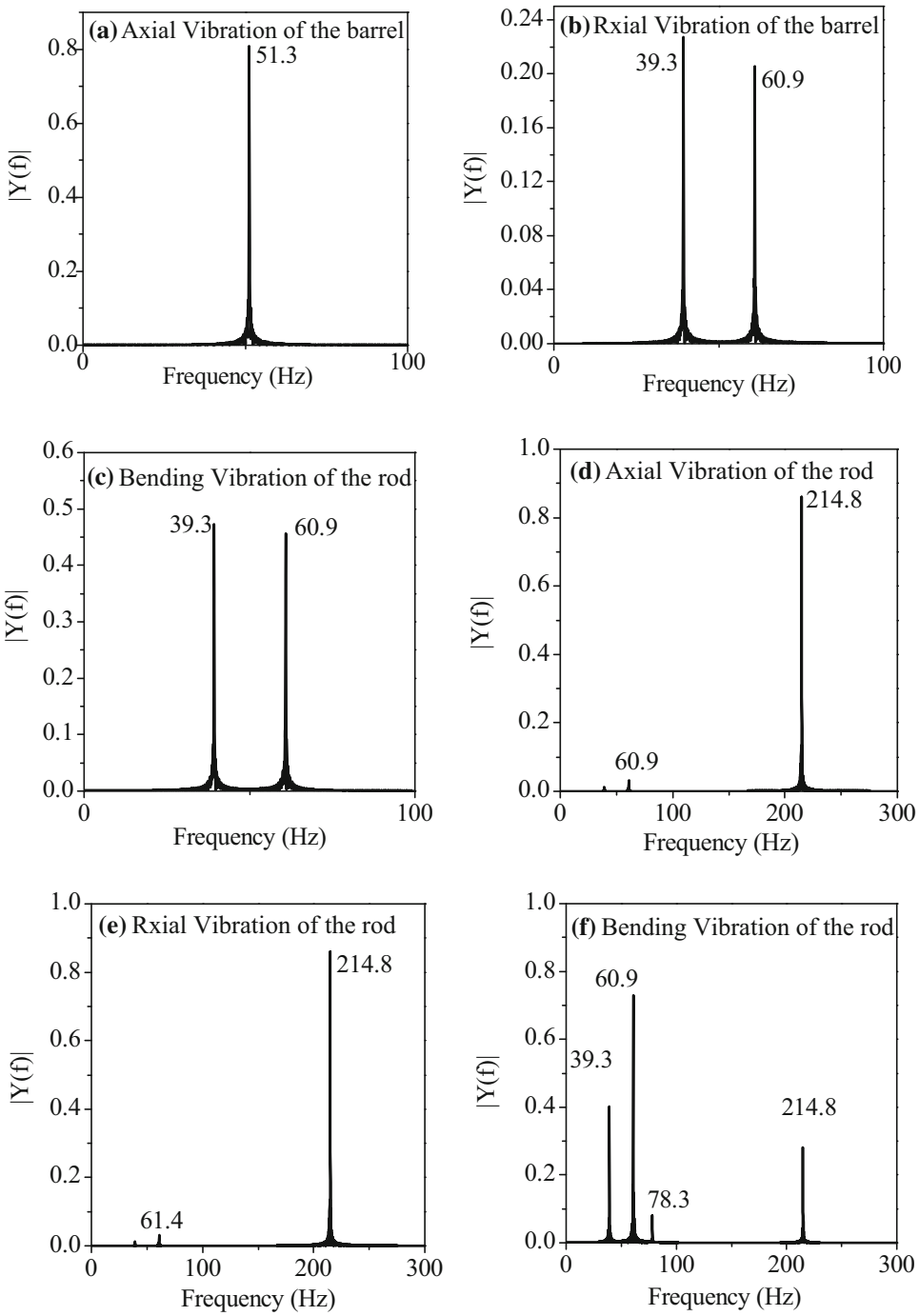

Figure 6 Frequency analysis for gripper cylinder

Subtract c_1 from the original signal $x(t)$ for further decomposition as

$$x(t) - c_1 = r_1, \tag{15}$$

where r_1 is the residual. Repeat the above steps until the residual r_n or the IMF c_n is small enough to less than a threshold, or r_n is a monotone function. Sum all the IMFs and the residual together to reconstitute the signal,

$$x(t) = \sum_{i=1}^{n} c_i + r_n. \tag{16}$$

A test signal with random noise is used to verify the ability of EMD method for time–frequency analysis. Suppose the test signal x with variable frequencies at different time is

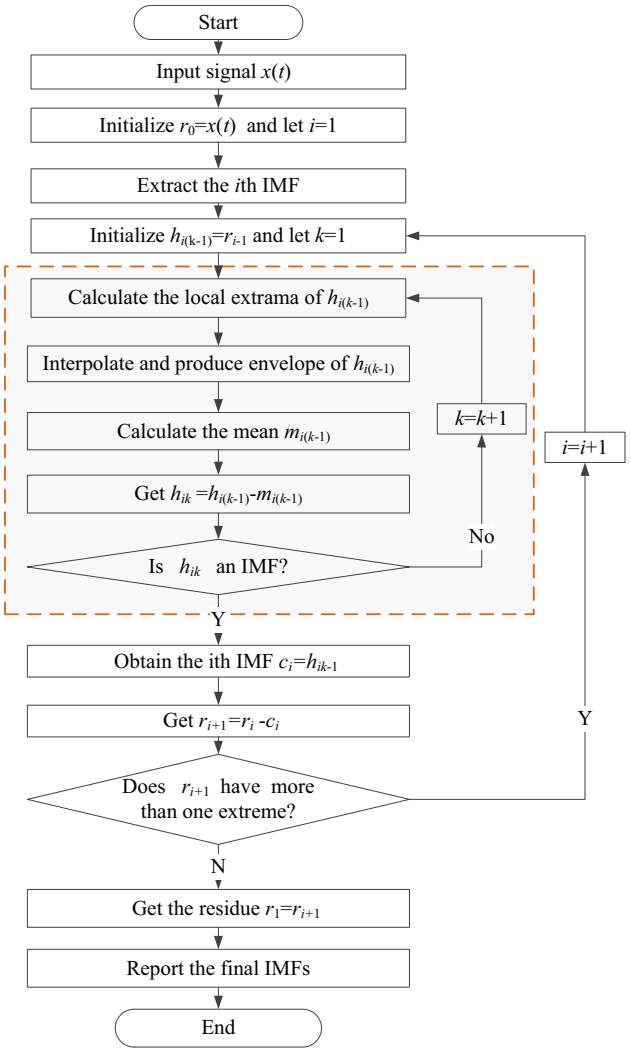

Figure 7 Flow chart of EMD method

$$\begin{cases} x = 2\sin(40\pi t) + 0.5\sin(60\pi t) + noise, & t \in [0, 2.5], \\ x = 2\sin(30\pi t) + 0.5\sin(20\pi t) + noise, & t \in (2.5, 5], \end{cases} \tag{17}$$

where *noise* is the random noise in the signal. The signal is decomposed into 7 IMFs with the EMD method and the results are shown in Figure 8(a). The original signal, the reconstructed signal and the reconstructed error are shown in Figure 8(b). The results show that the error between the original signal and the reconstructed signal is near to zero, which means that the IMFs obtained from the EMD method contains the most essence of the signal.

The frequencies in the signal could be detected by calculating the single-side spectrum of the decomposed IMFs with FFT and the result of every IMF is shown in Figure 9. The first IMF contains the main frequencies of

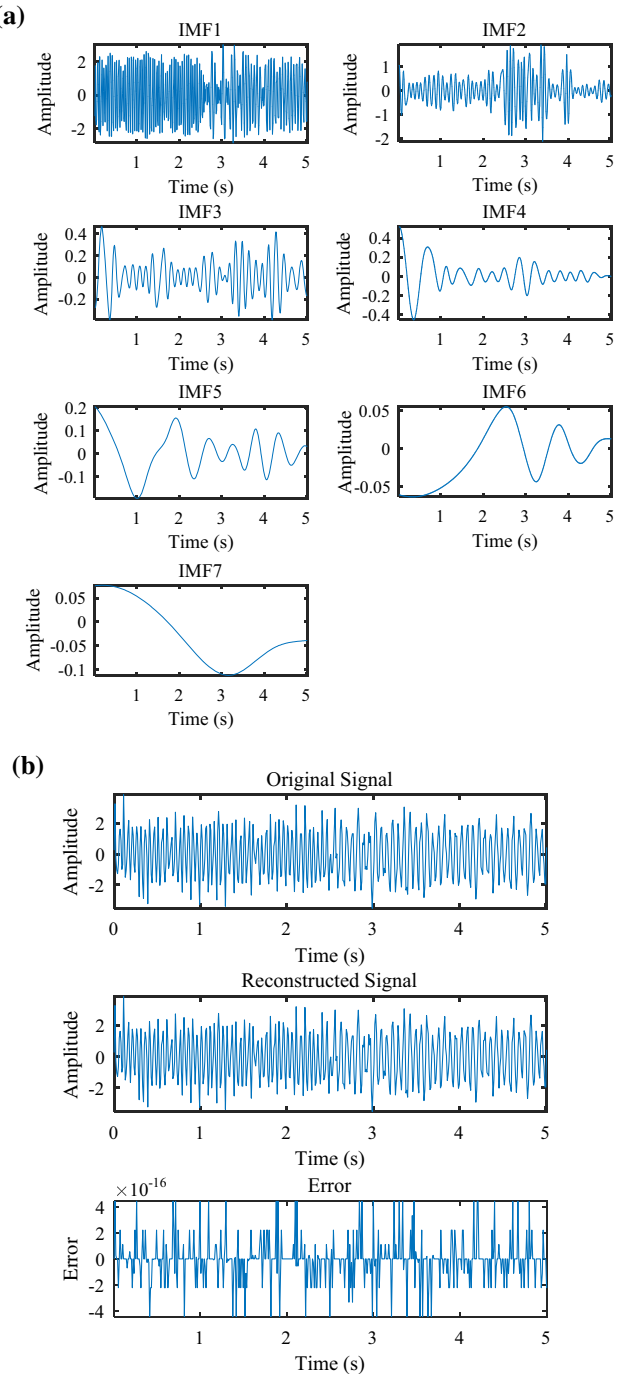

Figure 8 (**a**) Decomposed IMFs; (**b**) the original signal, the reconstructed signal and the reconstructed error of the signal

the original signal that are 15 Hz, 20 Hz and 30 Hz and the lowest frequency 10 Hz of the signal could be found in the second IMF. The frequencies could be obviously indicated with the application of EMD method although the noise in the signal makes the frequencies mixed with each other.

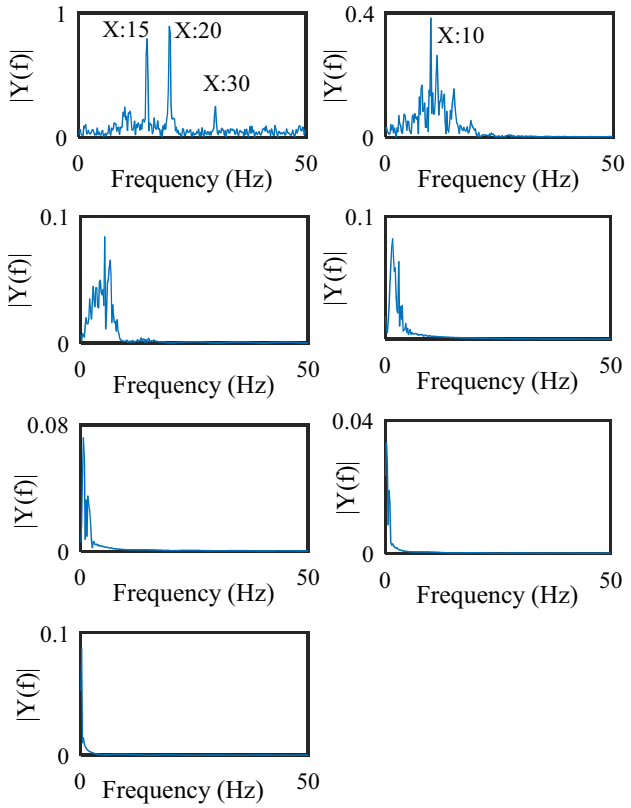

Figure 9 Single-side spectrum of the IMFs

4 Design of the Condition Monitoring System

4.1 Signal Processing on the Field Data

4.1.1 Frequency Analysis with FFT

A field test was conducted on one type of TBM working at normal condition to verify the lumped mass parameter model of the gripper cylinder. The tri-axial accelerators were mounted on the barrel of the gripper cylinder to measure the axial and transverse vibration signals of the cylinder. Meanwhile, the third axial was used to measure the vibration in the tunneling direction of TBM. The signals acquired from the accelerators settled on the gripper cylinder of TBM in the three directions were primarily analyzed with FFT to obtain the vibration frequencies of the gripper cylinder. The vibration signals in the time domain are shown in Figure 10(a) and the obtained frequencies are shown in Figure 10(b). The frequencies obtained from FFT are concentrated in the low frequency domain and the higher frequencies are buried in the signal that are hard to be detected. The result of the third channel that acquired the acceleration in the tunneling direction shows a frequency of 205.5 Hz that is near to theoretical natural frequency of the bending vibration of the piston rod

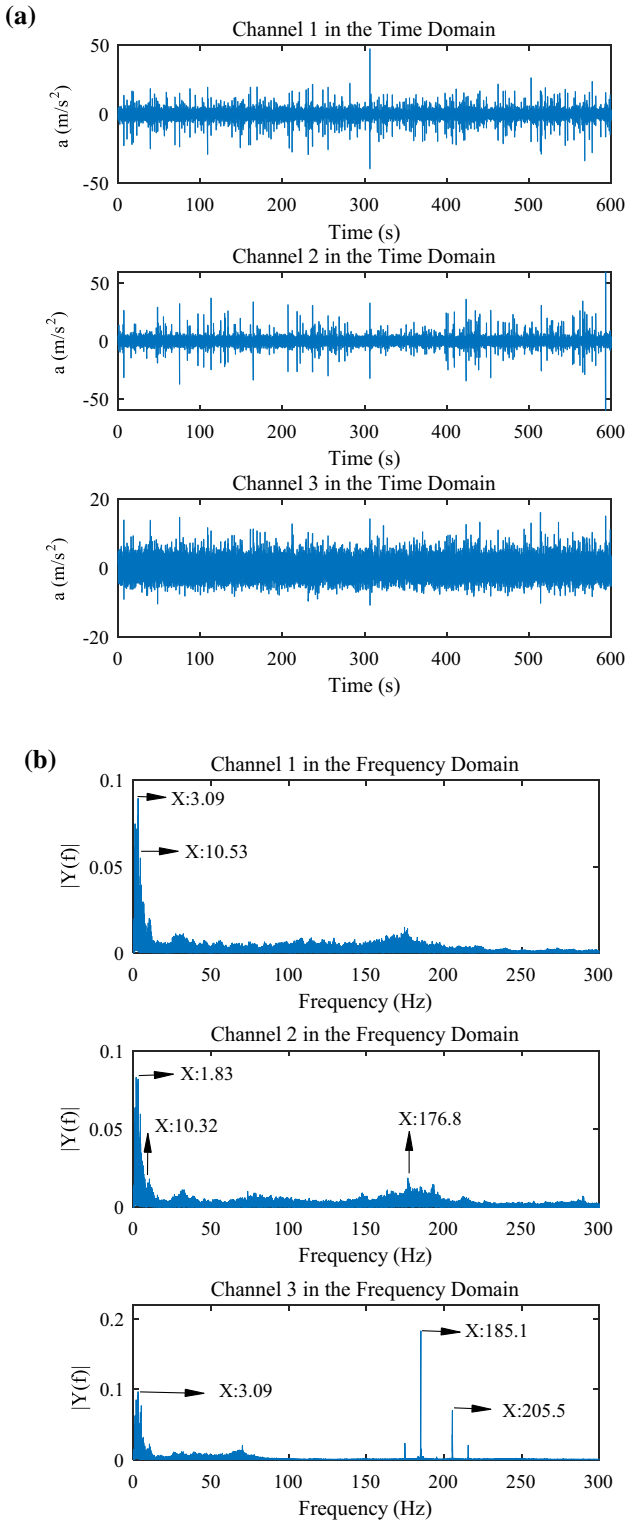

Figure 10 (**a**) Acceleration in different directions acquired from one TBM in time domain; (**b**) frequency obtained with FFT in frequency domain

of the gripper cylinder, however, the frequencies are mixed together and difficult to be indicated. The characteristic frequencies of the gripper cylinder are buried in the

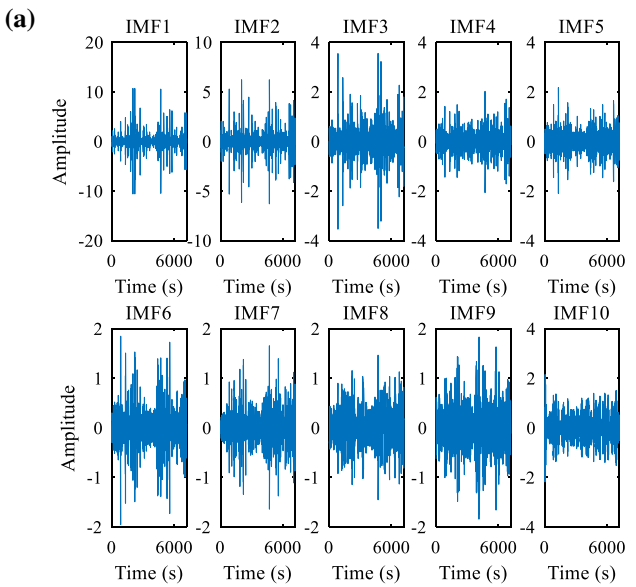

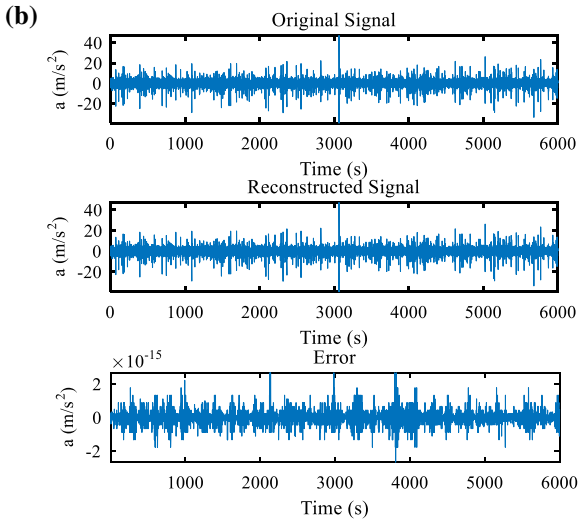

Figure 11 Reconstruction signal of IMFs by EMD method and original signal

complex vibration signals and they are hard to be detected with the FFT method. Hence, the EMD method was applied to indicate the characteristic frequencies of the gripper cylinder.

4.1.2 Frequency Analysis with EMD Method

The EMD method was used to decompose the vibration signals into IMFs to obtain the essence of the signal. Then the natural dynamic characteristics could be analyzed with the IMFs decomposed from the original signals. According to the algorithm of EMD method, the acceleration signals were decomposed into a serious of IMFs. There are 25

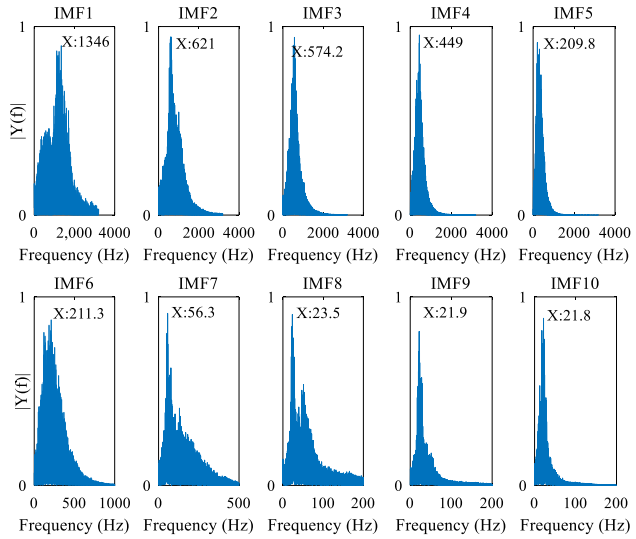

Figure 12 Frequencies of the IMFs

IMFs decomposed from the original signal with the designed threshold and the first 10 IMFs are shown in Figure 11(a) and the reconstructed signal can be obtained that is shown in Figure 11(b). The error between the original signal and the reconstructed signal is so small that could be neglected.

Simple-side spectra of the IMFs were used to calculate the frequencies of the acceleration signals. The first IMF includes the signal feature with the highest frequency of the signal and the following IMFs contain the lower frequencies with further decomposing in terms of the EMD algorithm. The first 10 IMFs were chosen to investigate the dynamic characteristics of the gripper cylinder because the frequencies of the further decomposed IMFs were near to zero and the results are illustrated in Figure 12. The frequencies of the IMFs obtained from the acceleration signals are from 21.83 Hz to 1346 Hz. The 51.46 Hz and 211.3 Hz could be found in IMF8 and IMF6 that are near to the theoretical natural frequencies of the axial vibration of the barrel and the bending vibration of the piston rod of the gripper cylinder, respectively. It means that the axial vibration of the barrel and the bending vibration of the piston rod of the gripper cylinder are the most intense vibration mode when the TBM works. The higher frequencies buried in the acceleration signals might be the natural frequencies induced by the rotor, the bearings, etc., or just the noises in the signal. The characteristic frequencies of the gripper cylinder could be indicated from the vibration signals acquired while TBM is working with application of EMD method, which proves the accuracy of the dynamic model and EMD method. Therefore, the online condition monitoring system based on the vibration signals could be performed.

4.2 Fault Diagnosis Based on the Dynamic Performance

4.2.1 The Equivalent Stiffness for the Contact Elements

The interaction between the barrel and CGS of gripper cylinder is equivalent as contact stiffness with the inner cylinder as shown in Figure 13, which can be calculated with the Hertz theory [23].

According to Hertz theory, the equivalent contact radius,R^*, of the curvature is defined as [24]

$$\frac{1}{R^*} = \frac{1}{R_1} + \frac{1}{R_2}, \tag{18}$$

where R_1 and R_2 are the radii of the barrel and CGS, respectively. The semi width, a, at the contact area could be expressed as [25]

$$a = \left[\frac{4PR_1R_2}{\pi l E^* \Delta R}\right]^{\frac{1}{2}}, \tag{19}$$

where ΔR is the difference of the deformation of the two contact components. E^* is the equivalent modulus of the elasticity of the two different materials, which is expressed as

$$E^* = \frac{1}{(1 - v_c^2/E_c) + (1 - v_c^2/E_b)}, \tag{20}$$

where E_c, v_c and E_b, v_b are Young's modulus, Poisson's rate of the CGS and the barrel, respectively. The relationship between the total deformation δ of the CGS and the barrel could be calculated with

$$\delta = \frac{P}{\pi E_c}\left[2\ln\left(\frac{4R_1}{a}\right) - 1\right] + \frac{P}{\pi E_b}\left[2\ln\left(\frac{4R_2}{a}\right) - 1\right]. \tag{21}$$

Then the stiffness at the interface between the CGS and the barrel could be expressed as [26]

$$k_s = \frac{\mathrm{d}P}{\mathrm{d}\delta} = \frac{\pi E}{2[\ln(\pi E^* \Delta R/P) - 1]}, \tag{22}$$

where P is the normal load. In addition, the equivalent stiffness between the seals and the barrel could be calculated with the same method.

The clearance at the contact interface would increase when the seals or the CGS have defects, thus the equivalent contact stiffness would change. The equivalent stiffness has negative correlation with the clearance as shown in Figure 14. Therefore, the equivalent stiffness would decrease when there are defects on seals or CGS in the cylinder.

4.2.2 Simulation of the Dynamic Performance with Different Equivalent Stiffness

The clearance at the contact interface would increase that would reduce their equivalent stiffness when the seals or the CGS has defects. Therefore, the dynamic performance of the gripper cylinder with variable stiffness is simulated. Moreover, the equivalent stiffness of the rock, the hydraulic oil, the seals and the CGS of the gripper cylinder varies in a range and the influences of the changing stiffness are investigated. The equivalent stiffness of the oil, the rock, the seals and CGS are varying in different ranges that are not in the same order of magnitudes. Hence, they are discretized as dimensionless equivalent stiffness to compare their influences on the natural frequency. The first order characteristic frequency of the gripper cylinder varying with the different equivalent stiffness is shown in Figure 15.

The natural frequency has positive correlation with the equivalent stiffness of the hydraulic oil, the seals, the CGS and the rock. Moreover, the relationships between the natural frequency and the variable equivalent stiffness are nonlinear because the different stiffness is coupled with

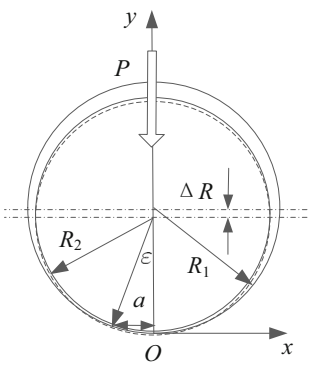

Figure 13 Scheme of two cylindrical surfaces in contact

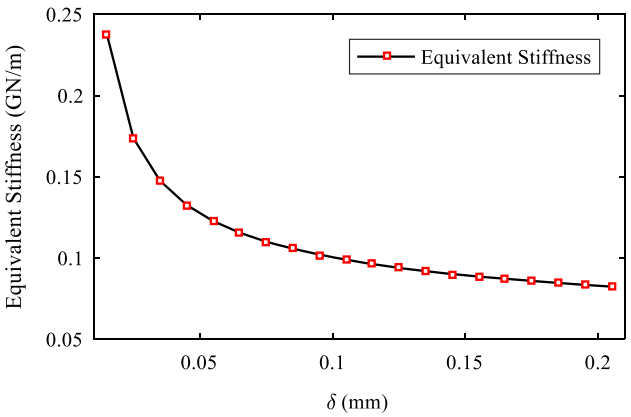

Figure 14 Relation between the deformation and the equivalent stiffness

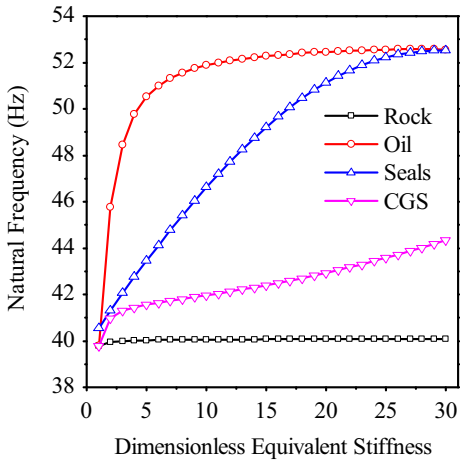

Figure 15 Nature frequency of the gripper cylinder changing with equivalent stiffness of the CGS, the oil, the seals and the extension of piston

each other. The natural frequency increases 33.3% with the equivalent stiffness of the seals changing from 0.01 GN/m to 0.15 GN/m and it also increases 33.3% when the equivalent stiffness of the oil changes from 0.3 GN/m to 1.2 GN/m. While the frequency increases 12.8% with the equivalent stiffness of the CGS changing from 0.2 GN/m to 6 GN/m. The nature frequency changes 1.1% when the equivalent stiffness of the rock varies from 20 GN/m to 120 GN/m. It can be concluded that the equivalent of the seals and the oil are the most effective parameters that influence the frequency of the gripper cylinder. The natural frequency of the cylinder that would change when the stiffness varies could be an indicator for fault diagnosis.

The natural frequency of the gripper cylinder would decrease with the degradation of the equivalent stiffness of the seals or the CGS according to the simulation of the lumped mass parameter model with different equivalent stiffness. It means that the natural frequency of the gripper cylinder would reflect the defects of the seals or the CGS. The EMD method could be used for data analysis of the monitoring vibration signals for evaluating the changes of the frequency as it is verified with the test signal. Therefore, failure could be indicated if a decrease of the natural frequency is detected and the online monitoring system based on vibration signals with EMD method could be established for health evaluation of the gripper cylinder.

4.3 Online Condition Monitoring System

Condition monitoring system is essential for complex mechanical systems [27]. The online condition monitoring system that consists of accelerators settled on the TBM, the data acquisition system and computer is shown in Figure 16. Several tri-axial accelerators are mounted on the barrel of the gripper cylinder to measure the acceleration in three directions. The x axial of the accelerator measures the acceleration in the axial direction of the cylinder, y axial is used to monitor the transverse vibration signal of the cylinder and z axial is defined as the tunneling direction. The vibration signals could be acquired through the data acquisition system and stored in computer.

The working flowchart of the monitoring system is shown in Figure 17. The acquired vibration data would be sent to the computer for data processing. The signal processing would be performed every propelling cycle and an alarm would be sent to the monitoring center when a fault occurs based on the dynamic model and the data analysis result.

Figure 16 Condition monitoring system

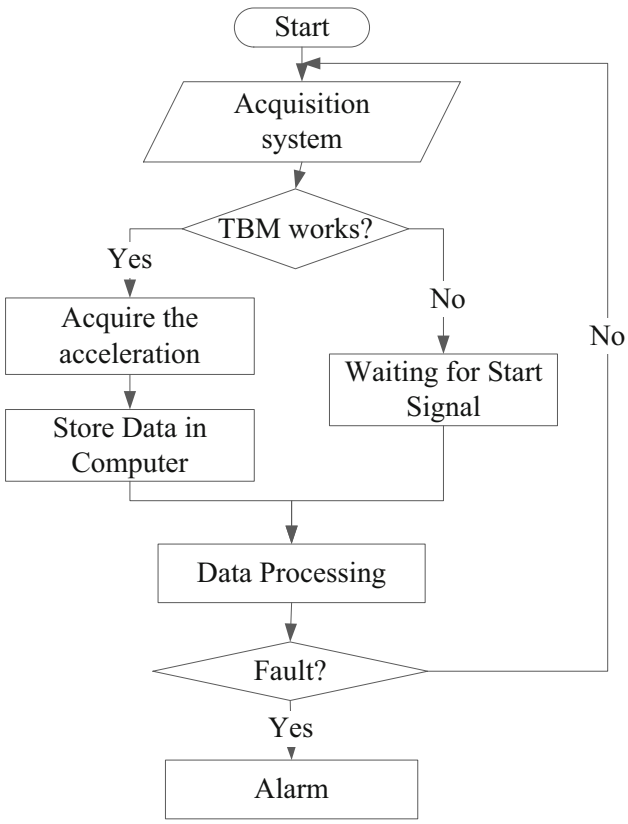

Figure 17 Flow chart of condition monitoring

5 Conclusions

Online condition monitoring for the gripper cylinder with application of EMD method is the main concern of this paper because the gripper cylinder is vulnerable to the vibration. A lumped mass parameter model with variable stiffness is established to investigate the vibration performance of the gripper cylinder in TBM. The stiffness at the interface between the CGS and barrel are calculated with the Hertz theory and it decreases with the increment of the clearance according to the simulation. Thus, the natural frequency would decrease if the seals or the CGS has defects based on the simulation of the dynamic performance with the decreased stiffness. The EMD method could indicate the characteristic frequencies from the complex vibration signals acquired from the working TBM. Consequently, an online condition monitoring system for the gripper cylinder of TBM based on the EMD method and the vibration signals is established. The failure could timely be detected that could ensure the safety of the TBM project.

References

1. J Z Huo, N Hou, W Sun, et al. Analyses of dynamic characteristics and structure optimization of tunnel boring machine cutter system with multi-joint surface. *Nonlinear Dynamics*, 2016: 1–18.
2. J Z Huo, W Z Wang, W Sun, et al. The multi-stage rock fragmentation load prediction model of tunnel boring machine cutter group based on dense core theory. *International Journal of Advanced Manufacturing Technology*, 2016: 1–13.
3. H Wu, J Huo, X Song, et al. The vibration analysis of TBM tunnelling parameters based on dynamic model. *Intelligent Robotics and Applications*, Springer International Publishing, 2015: 489–500.
4. K Zhang, H Yu, Z Liu, et al. Dynamic characteristic analysis of TBM tunnelling in mixed-face conditions. *Simulation Modelling Practice & Theory*, 2010, 18(7): 1019–1031.
5. W Sun, J X Ling, J Z Huo, et al. Dynamic characteristics study with multidegree-of-freedom coupling in TBM cutterhead system based on complex factors. *Mathematical Problems in Engineering*, 2013, 2013(3): 657–675.
6. X Zou, Y Mi, H Zheng, et al. Influence of vibration on the performance of tunnel boring machines. *IEEE/ASME International Conference on Mechatronic and Embedded Systems and Applications*, 2016: 1–6.
7. H Gao, L Liang, X Chen, et al. Feature extraction and recognition for rolling element bearing fault utilizing short-time Fourier transform and non-negative matrix factorization. *Chinese Journal of Mechanical Engineering*, 2015, 28(1): 96–105.
8. H Wang, K Li, H Sun, et al. Feature extraction method based on Pseudo-Wigner-Ville distribution for rotational machinery in variable operating conditions. *Chinese Journal of Mechanical Engineering*, 2011, 24(4): 661–668.
9. H Yang, B Gao, G Tian, et al. Transient-spatial pattern mining of eddy current pulsed thermography using wavelet transform. *Chinese Journal of Mechanical Engineering*, 2014, 27(4): 768–778.
10. N E Huang, Z Shen, S R Long, et al. The empirical mode decomposition and the Hilbert spectrum for nonlinear and non-stationary time series analysis. *Proceedings of the Royal Society A Mathematical Physical & Engineering Sciences*, 1998, 454(1971): 903–995.
11. Y Lei, J Lin, Z He, et al. A review on empirical mode decomposition in fault diagnosis of rotating machinery. *Mechanical Systems and Signal Processing*, 2013, 35(1–2): 108–126.
12. R T Rato, M D Ortigueira, A G Batista. On the HHT, its problems, and some solutions. *Mechanical Systems and Signal Processing*, 2008, 22(6): 1374–1394.
13. G Rilling, P Flandrin, P Goncalves. On empirical mode decomposition and its algorithms. *IEEE-EURASIP Workshop on Nonlinear Signal and Image Processing, IEEER*, 2003: 8–11.
14. Z Liu, Z Zhang. The improved algorithm of the EMD endpoint effect based on the mirror continuation. *The 8th International Conference on Measuring Technology and Mechatronics Automation, IEEE*, 2016: 792–795.
15. B Tang, S Dong, T Song. Method for eliminating mode mixing of empirical mode decomposition based on the revised blind source separation. *Signal Processing*, 2012, 92(1): 248–258.
16. J Yan, L Lu. Improved Hilbert–Huang transform based weak signal detection methodology and its application on incipient fault diagnosis and ECG signal analysis. *Signal Processing*, 2014, 98(5): 74–87.
17. M Zhang, T Jian, X Zhang, et al. Intelligent diagnosis of short hydraulic signal based on improved EEMD and SVM with few low-dimensional training samples[J]. *Chinese Journal of Mechanical Engineering*, 2016, 29(2): 396–405.
18. L Saidi, J B Ali, F Fnaiech, et al. Bi-spectrum based-EMD applied to the non-stationary vibration signals for bearing faults diagnosis. *Soft Computing and Pattern Recognition*, IEEE, 2015: 1650.
19. D H Pandya, S H Upadhyay, S P Harsha. Fault diagnosis of rolling element bearing with intrinsic mode function of acoustic emission data using APF-KNN. *Expert Systems with Applications*, 2013, 40(10): 4137–4145.
20. A S Raj, N Murali. Morlet wavelet UDWT De-noising and EMD based Bearing Fault Diagnosis. *Electronics*, 2013, 17(1): 1–8.
21. G Cheng,Y L Cheng, L H Shen, et al. Gear fault identification based on Hilbert–Huang transform and SOM neural network. *Measurement*, 2013, 46(3): 1137–1146.
22. G F Bin, J J Gao, J Li, et al. Early fault diagnosis of rotating machinery based on wavelet packets—Empirical mode decomposition feature extraction and neural network. *Mechanical Systems and Signal Processing*, 2012, 27(1): 696–711.
23. P Liu, H Zhao, K Huang, et al. Research on normal contact stiffness of rough surface considering friction based on fractal theory. *Applied Surface Science*, 2015, 349: 43–48.
24. C Brutti, G Coglitore, P P Valentini. Modeling 3D revolute joint with clearance and contact stiffness. *Nonlinear Dynamics*, 2011, 66(4): 531–548.
25. A Ghosh, B Leonard, F Sadeghi. A stress based damage mechanics model to simulate fretting wear of Hertzian line contact in partial slip. *Wear*, 2013, 307(1–2): 87–99.
26. R Buczkowski, M Kleiber, G Starzyński. Normal contact stiffness of fractal rough surfaces. *Archives of Mechanics*, 2014, 66(6): 411–428.
27. L Hu, N Hu, G Qin, et al. Turbopump condition monitoring using incremental clustering and one-class support vector machine. *Chinese Journal of Mechanical Engineering*, 2011, 24(3): 474–479.

Lin Li, born in 1989 is currently a PhD candidate at *State Key Laboratory of Mechanical System and Vibration, Shanghai Jiao Tong University, China.* She received her bachelor degree from *Southwest Jiaotong University, China*, in 2012. Her research interests include condition monitoring and fault diagnosis. Tel: +86-18818272950; E-mail: linli-sjtu@sjtu.edu.cn

Jian-Feng Tao, born in 1975, is currently an associate professor at *State Key Laboratory of Mechanical System and Vibration, Shanghai Jiao Tong University, China*. His research interests include intelligent hydraulic transmission and control technology and fault diagnosis. E-mail: jftao@sjtu.edu.cn

Hai-Dong Yu, born in 1975, is an associate professor at *Shanghai Key Laboratory of Digital Manufacture for Thin-walled Structures , China*. His research interests include dynamic performance and vibration analysis for complex engineering, damage mechanics. E-mail: hdyu@sjtu.edu.cn

Yi-Xiang Huang, born in 1980, is currently a research associate at *State Key Laboratory of Mechanical System and Vibration, Shanghai Jiao Tong University, China*. His research interests include big data, remote condition monitoring for mechanical engineering and PHM. E-mail: huang.yixiang@sjtu.edu.cn

Cheng-Liang Liu, born in 1964, is currently a professor and a PhD candidate supervisor at *State Key Laboratory of Mechanical System and Vibration, Shanghai Jiao Tong University, China*. His main research interests include remote monitoring for engineering, application of robots and intelligent agriculture equipment. E-mail: chlliu@sjtu.edu.cn